ANESTHESIOLOGY®

Anesthesia Workstation Performance in Pediatric Ventilation: Part 2. Characteristics during Pressure Support Ventilation and Oxygen Rise Times

Johannes Spaeth, M.D., Malte Trost, M.D., Bernd Flamm, Christin Wenzel, Ph.D., Stefan Schumann, Ph.D.

Anesthesiology 2026; 145:954–65

ABSTRACT

Background: Modern anesthesia workstations include various ventilator technologies, but the effects on pediatric ventilation are unclear. The hypothesis of this study was that performance during pressure support ventilation and times to increase oxygen concentrations depend on the type of anesthesia workstation.

Methods: Six modern anesthesia workstations (GE HealthCare Carestation 650; Mindray Bio-Medical Electronics Co. Ltd. Wato EX-65 Pro and A9; Dräger Medical Atlan A350 and Perseus A500; and Getinge Flow-c) were evaluated in respiratory models of a preterm baby, a neonate, an infant, and a toddler. Trigger response rates, trigger delay, and time to reach 50% of peak inspiratory pressure during pressure support ventilation were compared. Furthermore, the times required to increase oxygen concentration from 21 to 90% during pressure-controlled ventilation at fresh gas flows of 1, 3, and 10 l · min^{-1} were assessed in a compartment of the lung models with the volume corresponding to the respective model's functional residual capacity.

Results: Trigger response rates were above 90%, with few exceptions. Trigger delays ranged between 73 ± 6 and 145 ± 0 ms. Times to reach 50% peak pressure ranged between 161 ± 1 and 312 ± 1 ms, with decreasing variability in the larger patient models. Oxygen rise time varied between 94 ± 3 and 615 ± 60 s at the lowest fresh gas flow and decreased with increasing fresh gas flow to 3 l · min^{-1} and less so with further increasing fresh gas flow to 10 l · min^{-1}. Activation of oxygen flush did not generally increase oxygen concentration but caused relevant airway pressure increases in some devices.

Conclusions: Modern anesthesia workstations show an overall good performance during pressure support ventilation of children. During pressure-controlled ventilation, a moderate increase of fresh gas flow accelerated the rise in oxygen concentration, depending on the device. Oxygen flush brings no advantage in this regard but may put the patient at risk of high airway pressure.

(Anesthesiology 2026; 145:954–65)

EDITOR'S PERSPECTIVE

What We Already Know about This Topic

- Pressure support ventilation (PSV) is a most common available mode of supporting spontaneous breathing
- Technical efficiency of PSV is rated by the ventilator's response and pressure increase times
- Pediatric intensive care ventilators showed relevant differences in these measures depending on the ventilator type and technology of trigger detection
- Moreover, changes of gas concentration in anesthesia breathing circuits depend on fresh gas flow, internal volume of the breathing circuit, and ventilator technology to various extents

What This Article Tells Us That Is New

- A bench study of six modern anesthesia workstations using PSV in models for premature infants, neonates, infants, and toddlers found that most demonstrated good trigger response rates even at minimal trigger effort
- The trigger delay and pressurization varied considerably between devices
- Increasing fresh gas flow from 1 to 3 l · min^{-1} accelerated the rise of oxygen concentration more than a further increase to 10 l · min^{-1}, and activation of the oxygen flush during pressure-controlled ventilation did not generally accelerate an increase in oxygen concentration but resulted in high airway pressure in certain devices

Supplemental Digital Content is available for this article. Direct URL citations appear in the printed text and are available in both the HTML and PDF versions of this article. Links to the digital files are provided in the HTML text of this article on the Journal's Web site (www.anesthesiology.org). Andrew Davidson, M.B.B.S., M.D., served as Handling Editor for this article. Part of this work has been presented as oral presentations at the Annual Scientific Meeting of the Association of Pediatric Anaesthetists of Great Britain and Ireland in London, United Kingdom, May 24 to 26, 2023, and at the Annual Conference of the Society for Neonatology and Pediatric Intensive Care Medicine in Hamburg, Germany, June 15 to 17, 2023. Part of this work was also included in a poster presentation at the Annual Meeting of the German Society of Anesthesiology and Intensive Care Medicine (Deutschen Gesellschaft für Anästhesiologie und Intensivmedizin) in Düsseldorf, Germany, April 27 to 29, 2023.

Submitted for publication October 18, 2025. Accepted for publication May 4, 2026. Published online first on May 13, 2026.

 Anesthesiology 2026; 145:954–65. DOI: 10.1097/ALN.0000000000006150

Abbreviations: **AWS**, anesthesia workstation; **FIO_2**, fraction of inspired oxygen; **FRC**, functional residual capacity; **PCV**, pressure-controlled ventilation; **PEEP**, positive end-expiratory pressure; **PSV**, pressure support ventilation; **PTP**, pressure–time product

<zdoi;10.1097/ALN.0000000000006150>

Ventilating children during surgery puts high demands on the performance of the anesthesia workstation (AWS). Ventilator technology, characteristics of integrated pressure and flow sensors, and the breathing circuit volume determine the quality of ventilation.[1] Assisted spontaneous breathing bears the advantages of maintaining physiologic respiratory mechanics and providing further insights into the patient's current conditions by monitoring breathing frequency and strength. Pressure support ventilation (PSV) is probably the most common available mode of supporting spontaneous breathing with a modern AWS.[2] Technical efficiency of PSV is generally rated by the ventilator's response and pressure increase times.[3,4] Pediatric intensive care ventilators showed relevant differences in these measures depending on the ventilator type and technology of trigger detection.[4] Accordingly, it can be assumed that the efficiency of PSV during intraoperative pediatric ventilation depends on the type of AWS.

Oxygen concentration during ventilation is another factor needing consideration when ventilating children. The need for an adequate oxygen reserve during airway management and unforeseen intraoperative respiratory events must be carefully weighed up against the potentially harmful effects of high oxygen concentrations.[5,6] For this reason, it is recommended to reduce the inspiratory oxygen concentration to a minimum after securing the airway.[7,8] However, a sudden need to increase oxygen concentrations may then be time consuming. This time delay may depend on technical characteristics of the AWS, such as the type of ventilator and the principle of fresh gas supply.

Since little is known about the performance of modern AWS in these regards, we examined six AWSs for their trigger performances during PSV and the time required to increase alveolar oxygen concentration during pressure-controlled ventilation (PCV). The experiments were performed in physical models designed to mimic physiologic conditions of preterm babies, neonates, infants, and toddlers. We hypothesized that modern AWSs with various ventilator technologies differ in their performance of ventilation when parameters are set in the pediatric range.

Materials and Methods

Six modern AWSs were investigated: Carestation 650 (software version 2.00.01; GE HealthCare, USA), Wato EX-65 Pro (software version 05.05.00; Mindray Bio-Medical Electronics Co. Ltd., China), A9 (software version 01.17.00; Mindray), Atlan A350 (software version 2.00.01; Dräger Medical, Germany), Perseus A500 (software version 2.03; Dräger Medical), and Flow-c (software version 04.09.00; Getinge, Sweden). The included AWSs contain different types of ventilator technology: Tidal ventilation was driven by a bellow with the Carestation and the Wato, by a piston with the Atlan, by a turbine with the Perseus, and by a volume reflector with the Flow-c and the A9. According to manufacturers' specifications, each AWS has a specific system volume in the controlled ventilation mode (including recommended single-use absorber canister; approximated for the maximum volume of each ventilator unit): Wato EX-65 Pro (4,350 ml), Atlan A350 (3,440 ml), A9 (3,300 ml), Carestation 650 (3,006 ml), Flow-c (2,800 ml), and Perseus A500 (2,180 ml). For specifications on machine setup, please refer to the accompanying article.[9] Device-specific compliance tests and leakage tests were performed according to the manufacturers' advice before measurements with the respective breathing system in place.

Physical Patient Models

Model characteristics were adjusted to mimic the respiratory system of four different patient categories (with approximated body weight): preterm baby (about 2 kg), neonate (about 3.5 kg), infant (about 10 kg), and toddler (about 14 kg; fig. 1). Ventilation was simulated at targeted end-expiratory carbon dioxide partial pressure of 35 to 45 mmHg, measured in the AWSs. Single-use breathing systems were used with the size appropriate for the patient model in question. For simulated ventilation of preterm babies and neonates, 10-mm-inner-diameter breathing tubes were used (150 cm; reference No. 305/8173; Medtronic, Ireland) with a 0.5-l breathing bag attached. For simulated ventilation of infants and toddlers, 15-mm-inner-diameter breathing tubes were used (150 cm; reference No. 305/8926; Medtronic) with a 1.0 l breathing bag attached. Endotracheal tubes (Microcuff, Avanos Medical GmbH, Germany) of 3.0-, 3.5-, 4.0-, and 4.5-mm inner diameters were used for simulated ventilation of preterm babies, neonates, infants, and toddlers, respectively. No additional filters or heat and moisture exchanger were used to prevent the additional resistance from obscuring potential differences in the performance of the devices. More information on the model setup, as well as pressure and flow measurements, can be found in the accompanying article.[9]

Specific Model Setup: Trigger Performance and Pressurization

During PSV, triggering was realized using a custom-built piston pump, driven by a digitally controlled linear motor specifically programmed for this purpose (supplemental fig. S1, https://links.lww.com/ALN/E563; fig. 1D). Impulses for spontaneous breaths were given model specifically at random time intervals

Johannes Spaeth, M.D.: Department of Anesthesiology and Critical Care, Medical Center–University of Freiburg, Faculty of Medicine, University of Freiburg, Freiburg, Germany.

Malte Trost, M.D.: Department of Anesthesiology and Critical Care, Medical Center–University of Freiburg, Faculty of Medicine, University of Freiburg, Freiburg, Germany.

Bernd Flamm: Department of Anesthesiology and Critical Care, Medical Center–University of Freiburg, Faculty of Medicine, University of Freiburg, Freiburg, Germany.

Christin Wenzel, Ph.D.: Department of Anesthesiology and Critical Care, Medical Center–University of Freiburg, Faculty of Medicine, University of Freiburg, Freiburg, Germany.

Stefan Schumann, Ph.D.: Department of Anesthesiology and Critical Care, Medical Center–University of Freiburg, Faculty of Medicine, University of Freiburg, Freiburg, Germany.

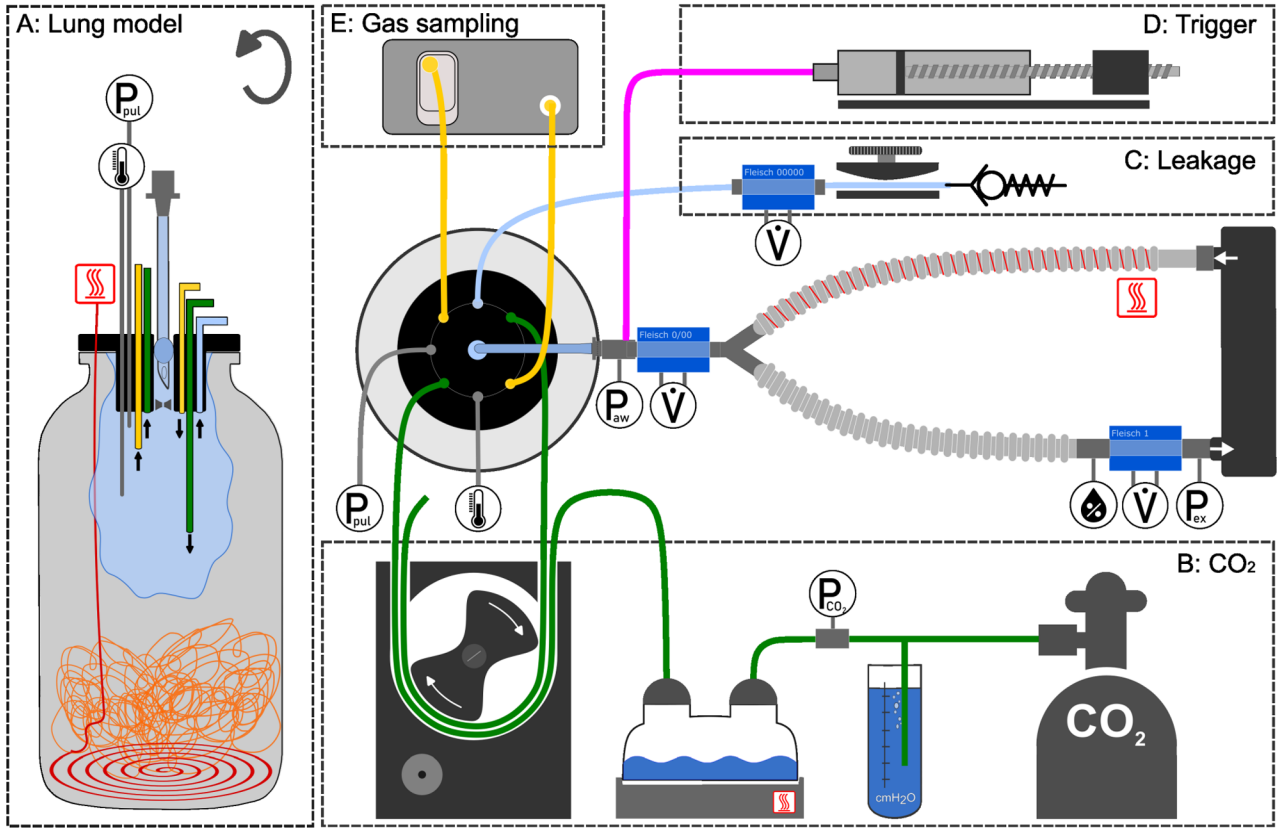

Fig. 1. Experimental setup. (*Left side*, *A*) Schematic drawing of the lung model simulated by a glass bottle with the volume corresponding to the respiratory system compliance of the simulated patient. The bottle includes a heating wire (*red*), copper wool (*orange*) and central opening for the endotracheal tube. Sealing of the bottle includes boreholes for lung pressure and temperature measurement, leakage outflow (*blue tube*), carbon dioxide (CO_2) inlet, and outlet (*green tubes*), as well as inlet and outlet for gas concentration measurements (*yellow tubes*). Please note the thin-walled plastic foil within the bottle (*bright blue*) separating the ventilated compartment from the bottle's volume without contributing to the compliance of the model. Moreover, tubes for inflow and outflow of CO_2 within the inner compartment end at different heights to ensure uniform gas mixing. (*Right side*) Lung model (bird's eye view) with the breathing system and anesthesia workstation attached to the endotracheal tube. Pressure (P), flow ($\dot{V}$), temperature, and humidity were measured at several points in the breathing circuit. Please note the heating wire (*red line*) around the inspiratory limb of the breathing system. (*B*) Technique of insufflation of CO_2 including cylinder, regulation of supply pressure (P_{CO_2}) to mean airway pressure with an underwater tube, moistening CO_2 with an active humidifier, and insufflation of CO_2 into the lung model using a roller pump. Please note that the tubes intended for inflow and outflow of CO_2 are inserted in opposite directions to ensure volume exchange in equal parts. (*C*) Throttle valve and mechanical positive end-expiratory pressure valve to regulate leakage flow according to the measured flow ($\dot{V}$). (*D*) Piston pump for the generation of trigger impulses. (*E*) Sidestream gas analyzer for the analysis of oxygen and CO_2 concentration within the inner compartment of the lung model.

(temporal pauses from end expiration to start inspiration: 0.01 to 3.0 s) to simulate spontaneous breathing variability. Time intervals for the impulse were constant: negative flow for 0.2 s, followed by a pause of 0.8 s, and slow piston return to starting position (0.8 s; positive flow). In preliminary experiments, negative trigger airway pressures (and corresponding flows) were determined as -1.0 ± 0.0 cm H_2O (-0.99 ± 0.01 l · min^{-1}) in the preterm baby model, -1.4 ± 0.1 cm H_2O (-1.34 ± 0.03 l · min^{-1}) in the neonate model, -1.2 ± 0.2 cm H_2O (-1.85 ± 0.01 l · min^{-1}) in the infant model, and -2.1 ± 0.0 cm H_2O (-2.07 ± 0.00 l · min^{-1}) in the toddler model. Flow rate, pressure, and an electronic signal of the trigger impulse were recorded synchronously at a sampling rate of 200/s to discriminate between simulated efforts and machine self-triggers. For experiments with PSV, breathing gas was conditioned targeting physiologic temperature and humidity. For examining the effects of leakage around an airway device, leakage was generated targeting 20% of delivered minute ventilation during volume-controlled ventilation.[9]

Protocol: Trigger Performance and Pressurization

For PSV, the inspiratory trigger of the AWS in question was set at the maximum sensitivity without causing

autotriggering before starting the experiments. The inspiratory pressure support was set to 6 cm H_2O above positive end-expiratory pressure (PEEP) of 5 cm H_2O, and inspiratory ramp and minimal ventilation frequency were switched off. Termination of inspiration was set to 25% of peak flow. Fresh gas flow was set to 0.5 l · min^{-1}, and fraction of inspired oxygen (F_{IO_2}) was set to 0.4. To mimic clinical use as much as possible, each measurement consisted of the following steps: disconnecting the breathing system; starting the recordings with the sensors open to ambient air; connecting the breathing system; starting the trigger pump; and starting PSV at the set parameters. The recordings were performed for a minimum of 2 min.

Trigger performance and pressurization were evaluated *via* established parameters.[2,3] Trigger response rate was determined as the ratio between breaths in response to the electronically detected trigger signal and all trigger signals during the interval. Trigger delay was defined as the time between the electronic trigger signal and the nadir of the pressure trace (fig. 2). Further, the pressure–time product (PTP), *i.e.*, the area under the airway pressure time curve, was determined for the interval of trigger delay, with lower values indicating less breathing effort. Moreover, in terms of performance on pressurization, the times required for pressure increase to 50% (T_{P50}) and 90% (T_{P90}) of the maximum airway pressure were determined, and the difference between trigger delay and T_{P50} was calculated. The time delay between the electronic trigger signal and the pneumatic consequence, *i.e.*, a measurable pressure drop at the site of the airway pressure sensor in the breathing model, was determined as 40 ms. All times on trigger performance were corrected respectively.

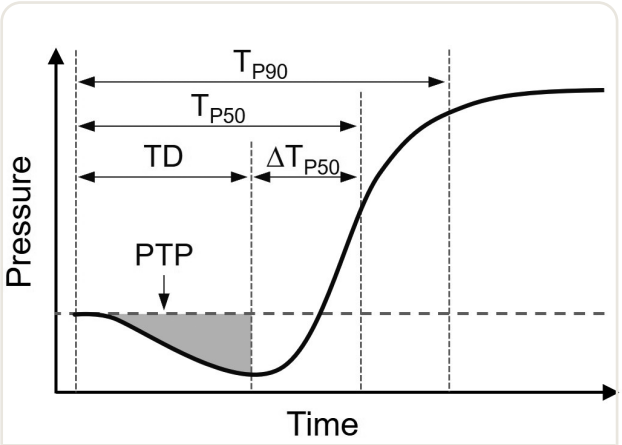

Fig. 2. Schematic drawing of the airway pressure curve with pressure support ventilation. *Vertical dashed lines* show time points for the assessment of trigger delay (T_D) and pressure at 50% (T_{P50}) and 90% (T_{P90}) of maximum airway pressure. ΔT_{P50} represents the time difference between T_{P50} and T_D. The *horizontal dashed line* indicates the positive end-expiratory pressure. The area bounded by T_D, positive end-expiratory pressure, and the airway pressure curve represents the pressure time product (PTP).

Specific Model Setup: Oxygen Rise Times

Oxygen concentration was measured within an inner compartment of the lung model corresponding to the functional residual capacity (FRC) of the respective patient category using a gas analyzer (Scio Four Oxi plus; Dräger, Germany; fig. 1E). To ensure volume consistency and thereby maintain homogeneous gas mixing, the sample gas was extracted in the lower part of the inner compartment and returned to the upper part with a flow rate of 200 ml · min^{-1}. The delay of the gas analyzer was determined to be 6.5 s in preliminary experiments. Time-based results were corrected accordingly.

Protocol: Oxygen Rise Times

During PCV, the oxygen concentration rise time from 21 to 90% was determined. Ventilation frequencies were set to 40/min, 35/min, 30/min, and 25/min in the preterm baby, neonate, infant, and toddler models, respectively. PEEP was set to 5 cm H_2O, inspiratory to expiratory ratio was set to 1:2, and peak inspiratory pressure was set to 6 cm H_2O above PEEP in all models.

For the measurements, the inner compartment of the lung model was evacuated. F_{IO_2} was set to 0.21. The lung model was connected to the breathing circuit to generate a volume within the inner compartment corresponding to the functional residual capacity, and the lung models were pressurized with constant 5 cm H_2O in the beginning of the experiment to generate volumes within the FRC of approximately 50, 90, 250, and 350 ml for the preterm baby, neonate, infant, and toddler models, respectively. Subsequently, F_{IO_2} was set to 1.0, and ventilation was switched to PCV. Measurements were performed at fresh gas flows of 1, 3, and 10 l · min^{-1} and with activated oxygen flush.

During measurements on the oxygen flush function, a fresh gas flow of 1 l · min^{-1} and a F_{IO_2} of 0.21 were set, and the oxygen flush button was pushed continuously. Pressure, flow, and gas concentrations were recorded until 90% oxygen concentration was reached or, if no changes were detected, after a minimum of 60 s. Three measurements were performed for each measurement after complete dismantling and rebuilding of the setup.

Data Analyses and Statistics

The data were analyzed using MATLAB (version R2019a; MathWorks Inc., USA) and GraphPad Prism (version 9.0.2; GraphPad Software Inc., USA). The results are expressed as means ± SD based on the three repetitions of the experiments; no statistical comparisons are presented.

Results

Trigger Response Rate

During PSV, the Carestation, the Perseus and the Flow-c responded to patient trigger in more than 90% of the

given breathing efforts with all patient models without leakage (table 1). In the other devices, the minimum response rate without leakage was 69 ± 7% in the Wato, 81 ± 3% in the Atlan, and 39 ± 5% in the A9, whereas in the A9, most failed triggers occurred in the preterm baby model. Trigger efforts without response were often associated with trigger impulses in quick succession. The presence of a leak reduced the percentage of trigger

Table 1. Trigger Performance and Pressurization during Pressure Support Ventilation without and with Leakage Depending on the Patient Model and Type of Anesthesia Workstation

Workstation in Patient Model	Leakage	Resp., %	T_D, ms	T_{P50}, ms	T_{P90}, ms	ΔT_{P50}, ms	PTP, cm H_2O · ms
Preterm baby							
Carestation	Without	100 ± 0	145 ± 0	189 ± 0	208 ± 0	44 ± 0	−56 ± 1
	With	100 ± 0	137 ± 2	183 ± 3	203 ± 3	46 ± 0	−51 ± 1
Wato	Without	98 ± 2	102 ± 2	188 ± 1	247 ± 1	86 ± 2	−26 ± 1
	With	99 ± 2	113 ± 5	192 ± 2	253 ± 2	79 ± 3	−33 ± 2
Atlan	Without	81 ± 3	73 ± 6	178 ± 1	219 ± 2	104 ± 7	−14 ± 2
	With	70 ± 3	75 ± 5	183 ± 9	228 ± 11	113 ± 1	−12 ± 3
Perseus	Without	98 ± 4	118 ± 2	257 ± 3	289 ± 3	138 ± 1	−32 ± 1
	With	100 ± 0	123 ± 2	252 ± 2	285 ± 1	128 ± 4	−34 ± 1
Flow-c	Without	100 ± 0	110 ± 0	163 ± 1	274 ± 2	53 ± 1	−31 ± 1
	With	100 ± 0	97 ± 2	150 ± 1	260 ± 0	53 ± 2	−22 ± 1
A9	Without	39 ± 5	128 ± 2	309 ± 5	405 ± 4	180 ± 4	−41 ± 2
	With	42 ± 7	135 ± 4	306 ± 1	403 ± 1	171 ± 5	−47 ± 1
Neonate							
Carestation	Without	100 ± 0	120 ± 0	170 ± 0	193 ± 1	50 ± 0	−69 ± 2
	With	100 ± 0	110 ± 0	159 ± 2	184 ± 2	49 ± 2	−55 ± 1
Wato	Without	100 ± 0	120 ± 4	215 ± 2	278 ± 2	95 ± 3	−78 ± 6
	With	97 ± 5	112 ± 2	205 ± 2	268 ± 2	95 ± 5	−55 ± 4
Atlan	Without	94 ± 3	87 ± 6	198 ± 11	243 ± 4	111 ± 9	−31 ± 5
	With	96 ± 4	90 ± 11	204 ± 4	247 ± 3	114 ± 12	−32 ± 10
Perseus	Without	99 ± 2	133 ± 2	238 ± 3	264 ± 6	105 ± 2	−71 ± 2
	With	100 ± 0	132 ± 2	233 ± 3	262 ± 7	102 ± 3	−67 ± 2
Flow-c	Without	100 ± 0	103 ± 2	168 ± 1	284 ± 0	64 ± 2	−50 ± 2
	With	100 ± 0	88 ± 2	155 ± 1	276 ± 1	67 ± 1	−32 ± 1
A9	Without	94 ± 0	138 ± 6	312 ± 1	414 ± 1	174 ± 7	−86 ± 5
	With	94 ± 0	140 ± 4	312 ± 1	415 ± 2	172 ± 5	−85 ± 5
Infant							
Carestation	Without	100 ± 0	107 ± 2	161 ± 1	305 ± 5	54 ± 1	−70 ± 3
	With	99 ± 2	92 ± 2	143 ± 1	290 ± 3	52 ± 2	−49 ± 3
Wato	Without	92 ± 2	137 ± 2	240 ± 9	313 ± 7	104 ± 9	−124 ± 5
	With	82 ± 5	118 ± 8	209 ± 2	289 ± 1	91 ± 8	−76 ± 12
Atlan	Without	100 ± 0	107 ± 2	245 ± 2	355 ± 2	138 ± 1	−72 ± 5
	With	85 ± 5	125 ± 4	260 ± 6	364 ± 6	135 ± 8	−85 ± 3
Perseus	Without	100 ± 0	135 ± 0	232 ± 2	257 ± 2	97 ± 2	−95 ± 1
	With	100 ± 0	135 ± 0	223 ± 3	247 ± 2	88 ± 2	−93 ± 1
Flow-c	Without	100 ± 0	113 ± 2	209 ± 1	324 ± 3	95 ± 3	−75 ± 4
	With	100 ± 0	82 ± 2	194 ± 0	305 ± 2	112 ± 2	−34 ± 2
A9	Without	92 ± 7	125 ± 0	262 ± 1	367 ± 2	136 ± 1	−89 ± 1
	With	89 ± 2	125 ± 0	259 ± 4	362 ± 3	133 ± 3	−82 ± 1
Toddler							
Carestation	Without	91 ± 2	125 ± 0	194 ± 1	336 ± 2	69 ± 0	−135 ± 1
	With	83 ± 0	98 ± 2	188 ± 1	314 ± 0	89 ± 2	−79 ± 6
Wato	Without	69 ± 7	137 ± 2	247 ± 3	334 ± 3	110 ± 3	−162 ± 5
	With	63 ± 6	122 ± 5	225 ± 4	321 ± 1	103 ± 6	−118 ± 8
Atlan	Without	89 ± 2	115 ± 4	257 ± 1	365 ± 5	142 ± 4	−111 ± 7
	With	82 ± 7	128 ± 6	277 ± 6	385 ± 6	149 ± 2	−130 ± 12
Perseus	Without	98 ± 2	133 ± 2	240 ± 3	266 ± 3	107 ± 3	−136 ± 4
	With	100 ± 0	135 ± 0	225 ± 2	249 ± 3	90 ± 2	−132 ± 1
Flow-c	Without	100 ± 0	90 ± 0	210 ± 1	327 ± 0	120 ± 0	−66 ± 3
	With	94 ± 0	85 ± 0	216 ± 2	331 ± 2	131 ± 1	−51 ± 3
A9	Without	93 ± 2	125 ± 0	286 ± 3	386 ± 0	161 ± 2	−124 ± 1
	With	94 ± 0	123 ± 2	280 ± 1	383 ± 1	156 ± 2	−119 ± 4

Carestation, GE HealthCare, USA; Wato, Mindray Bio-Medical Electronics Co. Ltd., China; Atlan, Dräger Medical, Germany; Perseus, Dräger Medical; Flow-c, Getinge, Sweden; A9, Mindray.

PTP, pressure–time product; Resp., response rate; T_D, trigger delay; T_{P50}, time to pressurization of 50% of maximum airway pressure; T_{P90}, time to pressurization of 90% of maximum airway pressure; ΔT_{P50}, difference between T_D and T_{P50}.

response rate in some devices, particularly in the larger lung models.

Trigger Delay

The trigger delays ranged between 73 ± 6 ms (Atlan) and 145 ± 0 ms (Carestation). Leakage reduced trigger delay in most devices to a minor extent (fig. 3).

The 50% pressure rise time was shortest with the Flow-c in the preterm baby and the neonate models and with the Carestation in the infant and the toddler models, without leakage (fig. 3). The 50% pressure rise time was longest with the A9 with all tested models. Leakage had no relevant impact.

The differences between trigger delay and pressure rise time were comparable between different lung models per tested device. The mean difference for all lung models without leakage was lowest in the Carestation (54 ± 9 ms), followed by the Flow-c (83 ± 27 ms), the Wato (99 ± 11 ms), the Perseus (112 ± 17 ms), the Atlan (124 ± 18 ms), and the A9 (162 ± 18 ms; table 1). The PTP varied considerably between devices and increased with increasing lung model volume (table 1).

Oxygen Rise Time

During PCV, the times to increase simulated alveolar oxygen concentration to 90% varied considerably between devices, lung models, and fresh gas flow (table 2). At fresh gas flow of 1 l · min^{-1} 90%, oxygen concentration was achieved the fastest in the preterm baby model with the A9 (145 ± 3 s), in the neonate model with the Carestation (94 ± 3 s), and in the infant (364 ± 7 s) and the toddler model (306 ± 9 s) with the Flow-c.

In the preterm baby and the neonate model, increasing fresh gas flow from 1 to 10 l · min^{-1} decreased the oxygen rise time the most in the Perseus (mean decrease: 495 s) but considerably less so in all other devices (mean decrease: 59 s). In the infant and the toddler models, increasing fresh gas flow from 1 to 10 l · min^{-1} decreased the oxygen rise times in all devices (mean decrease: 200 s). In most devices, the rise of oxygen concentration was sped up more with an increase in fresh gas flow from 1 to 3 l · min^{-1} compared to an increase from 3 to 10 l · min^{-1}, particularly in the infant and toddler models (supplemental fig. S2, https://links.lww.com/ALN/E564).

The oxygen flush function did not generally reduce time to reach 90% oxygen concentration compared to increasing fresh gas flow from 1 to 10 l · min^{-1}. In terms of respiratory mechanics, activation of the oxygen flush resulted in a relevant initial increase in airway pressures compared to baseline ventilation in the Carestation, the Wato, and the A9 and a relevant initial increase in PEEP in the A9 but continuous increase in PEEP in the Carestation (fig. 4; supplemental table S1, https://links.lww.com/ALN/E562). No relevant changes were observed in the Atlan and the Perseus. In the Flow-c, cyclic ventilation was interrupted during the oxygen flush. Therefore, oxygen rise times and respiratory mechanics could not be analyzed in this device.

Discussion

The main findings of the current study are (1) most anesthesia workstations demonstrated good trigger response rates even at minimal trigger effort; (2) trigger delay and pressurization varied considerably between devices during

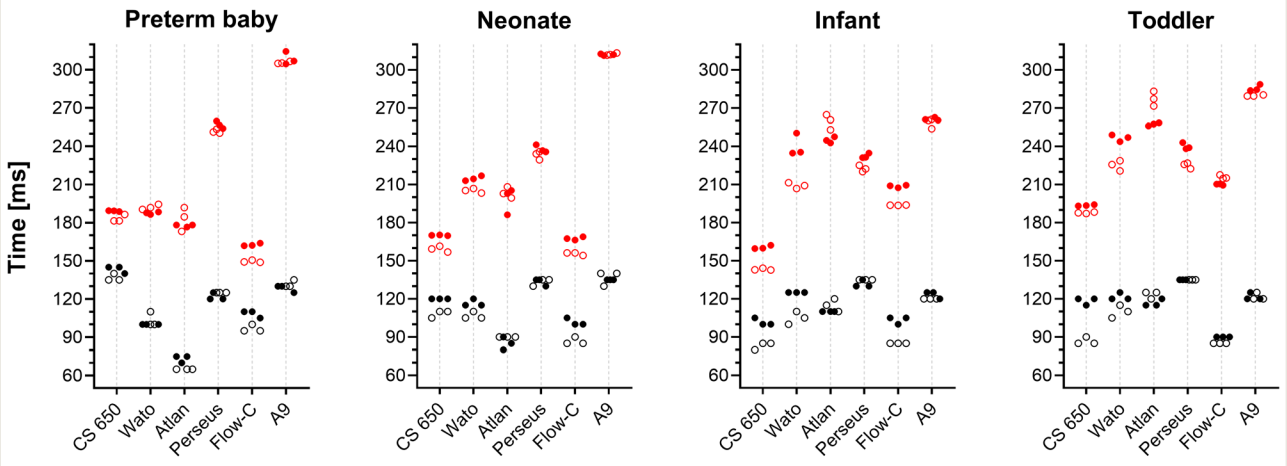

Fig. 3. Trigger performance and pressurization for different patient models (from *left* to *right*) and anesthesia workstations (*x-axis*) during pressure support ventilation. Trigger delay without leakage (*filled black dots*) and with leakage (*open black dots*); Time at 50% maximum airway pressure without leakage (*filled red dots*) and with leakage (*open red dots*). Symbols indicate a single measurement. (CS [Carestation] 650, GE HealthCare, USA; Wato EX-65, Mindray Bio-Medical Electronics Co. Ltd., China; Atlan A350, Dräger Medical, Germany; Perseus A500, Dräger Medical; Flow-C, Getinge, Sweden; A9, Mindray.)

Table 2. Time to Increase Oxygen Concentration in the Lung Models from 21 to 90% at 1, 3, and 10 l · min^{-1} Fresh Gas Flow, as Well as during Activation of the Oxygen Flush Function during Pressure-controlled Ventilation

	Oxygen Rise Time, s			
Workstation in Patient Model	**1 l · min^{-1}**	**3 l · min^{-1}**	**10 l · min^{-1}**	**O_2 Flush**
Preterm baby				
Carestation	149 ± 2	136 ± 1	127 ± 14	378 ± 31
Wato	188 ± 5	159 ± 4	164 ± 6	192 ± 10
Atlan	442 ± 10	400 ± 35	432 ± 29	299 ± 48
Perseus	615 ± 60	131 ± 3	120 ± 11	136 ± 31
Flow-c	228 ± 30	245 ± 13	195 ± 8	NA
A9	145 ± 3	138 ± 9	129 ± 5	130 ± 3
Neonate				
Carestation	94 ± 3	78 ± 1	59 ± 1	101 ± 5
Wato	133 ± 1	117 ± 1	113 ± 2	152 ± 2
Atlan	214 ± 20	170 ± 11	155 ± 4	120 ± 2
Perseus	562 ± 32	86 ± 2	64 ± 2	65 ± 2
Flow-c	100 ± 2	88 ± 4	93 ± 2	NA
A9	126 ± 3	113 ± 1	114 ± 3	116 ± 1
Infant				
Carestation	474 ± 17	101 ± 7	96 ± 7	338 ± 76
Wato	551 ± 12	111 ± 17	108 ± 6	190 ± 6
Atlan	598 ± 31	139 ± 1	123 ± 3	127 ± 6
Perseus	568 ± 16	129 ± 4	103 ± 2	133 ± 19
Flow-c	364 ± 7	153 ± 4	160 ± 4	NA
A9	399 ± 4	100 ± 9	92 ± 10	135 ± 9
Toddler				
Carestation	476 ± 74	63 ± 5	79 ± 2	288 ± 112
Wato	535 ± 10	46 ± 4	48 ± 1	98 ± 7
Atlan	540 ± 6	98 ± 2	82 ± 1	83 ± 2
Perseus	574 ± 40	123 ± 15	69 ± 7	84 ± 2
Flow-c	306 ± 9	58 ± 1	65 ± 3	NA
A9	388 ± 8	56 ± 1	48 ± 1	54 ± 1

The data are given as means ± SD. Carestation, GE HealthCare, USA; Wato, Mindray Bio-Medical Electronics Co. Ltd., China; Atlan, Dräger Medical, Germany; Perseus, Dräger Medical; Flow-c, Getinge, Sweden; A9, Mindray.

NA, not applicable.

PSV; (3) during PCV, increasing fresh gas flow from 1 to 3 l · min^{-1} accelerated the rise of oxygen concentration more than a further increase to 10 l · min^{-1}; and (4) activation of the oxygen flush during PCV did not generally accelerate an increase in oxygen concentration but resulted in high airway pressure in certain devices and interrupted ventilation in the Flow-c.

The model developed for the specific purpose of this study aimed at achieving the best approximation to physiologic conditions in the targeted patient group. Whereas glass bottles filled with copper wool and artificial resistances have been used to simulate respiratory system conditions in several studies with excellent quality,[10,11] this is the first model study working with humidified breathing gas in an experimental setup for semiclosed ventilation, to our knowledge.

Simulating irregular trigger impulses allowed us to determine trigger response rates beyond device-specific trigger thresholds. We are not aware of other bench studies having investigated neonatal ventilators in this regard during invasive assisted ventilation. The trigger response rates found in our study would be most comparable to clinical data reflecting patient–ventilator asynchrony. Patient–ventilator asynchrony is extremely common in mechanically ventilated children, and the predominant cause is ineffective triggering.[12] In contrast, most of the tested AWSs in our study detected breathing efforts with high reliability. Similar to the highly variable efficiency of flow trigger settings in mechanically ventilated neonates and children,[13] we found no systematic correlation between ventilator type, flow sensor, and trigger response rate. For example, both the Wato and the A9 use differential pressure sensors for flow measurement, but with the A9, the majority of breathing efforts were not detected in the preterm baby model. Our analyses revealed that the majority of failed responses followed shortly after responded triggers. Moreover, trigger response rates were superior with the Perseus compared to with the Atlan, although both machines use hot-wire anemometry. The Atlan simultaneously uses a pressure trigger to discriminate a breathing effort from flow artefacts. We assume that the low trigger flows in our experiments did not translate into sufficient pressure changes, confirming a genuine inspiratory effort.

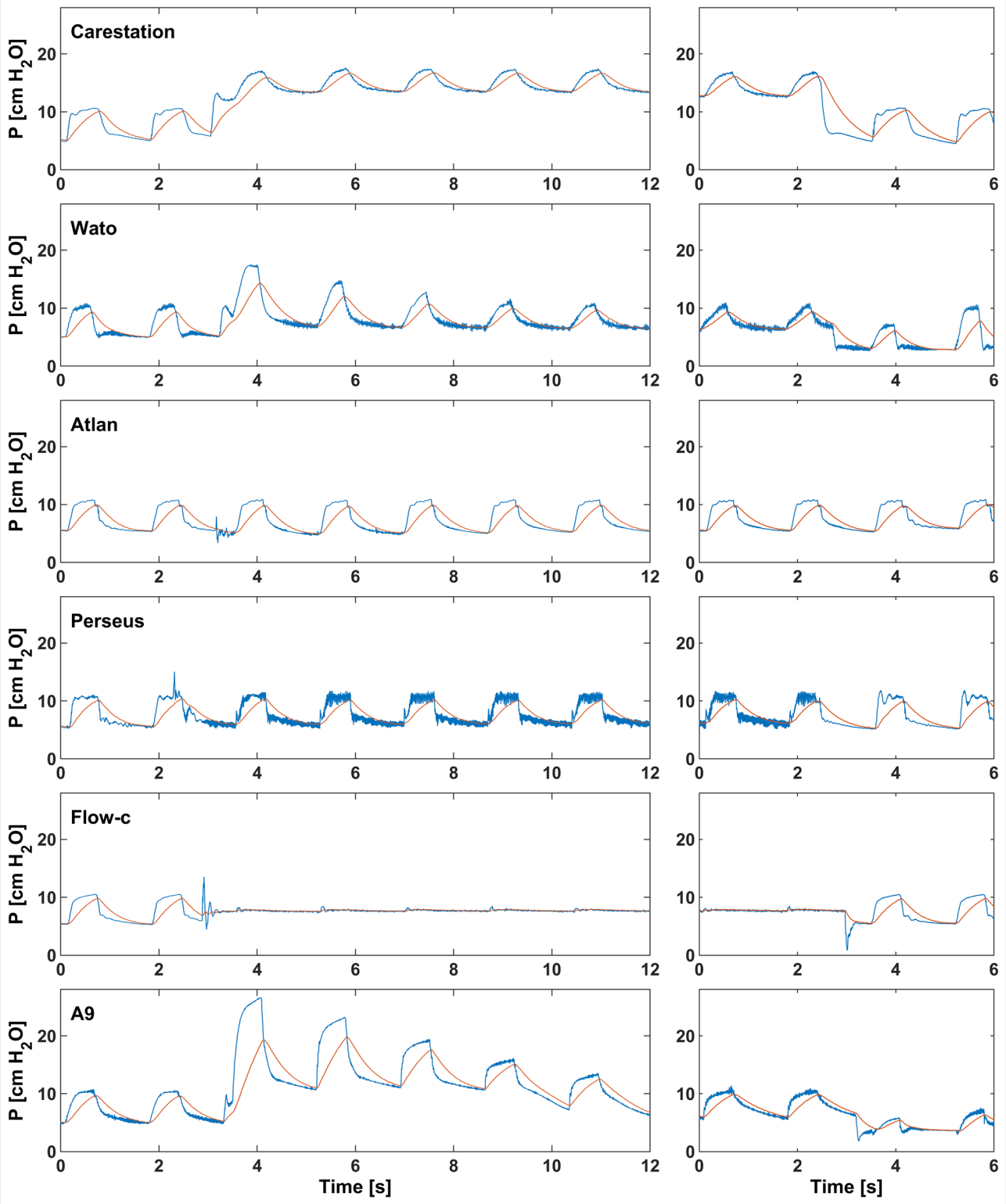

Fig. 4. Respiratory mechanics during activation of the oxygen flush function during pressure-controlled ventilation. Exemplary airway pressure (*blue*) and pulmonary pressure (*red*) curves for the onset of oxygen flush (*left panels*) and the end of oxygen flush (*right panels*) in the neonate patient model at a fresh gas flow of 1 l · min^{-1}. The oxygen flush button was pressed at time 0, kept pressed until oxygen concentration in the neonatal patient model reached 90% or did not change within 60 s during pressure-controlled ventilation (ventilation frequency of 35/min, positive end-expiratory pressure of 5 cm H_2O, and inspiratory pressure of 6 cm H_2O), and released thereafter (between 2 and 4 s in the *curves*). (Carestation, GE HealthCare, USA; Wato, Mindray Bio-Medical Electronics Co. Ltd., China; Atlan, Dräger Medical, Germany; Perseus, Dräger Medical; Flow-c, Getinge, Sweden; A9, Mindray.)

Interestingly, lower trigger response rates also occurred in the toddler model, although absolute trigger flow was higher. We attribute this difference to the larger volume of compressible breathing gas in the respiratory system. Higher compliance of the larger systems may attenuate the transmission of the trigger signal. In this regard, flow sensors positioned close to the patient, as available in some intensive care ventilators, may be advantageous.

Delay of trigger response varied between AWS and lung models. This measure depends on the sensitivity of the respective flow sensors and the device's ability to regulate pressurization. Pressurization of the breathing system starts before we are able to detect the machine's response in the airway pressure signal. High airway resistance counteracts the pressurization and may therefore explain the observed greater variability of trigger delay in the smaller patient models.

Times for trigger delay corresponded to the ranges found in intensive care ventilators intended for use with adult patients, pediatric patients, and neonates,[4] although some authors estimate the best performance being less than 100 ms.[14] In this regard, only the Flow-c met this criterion in all models. The performance of the other AWSs can be considered appropriate for the intended application for specific patient categories only. The comparison with respirators for specific use in neonates and infants shows, however, that trigger delay can be as low as 40 ms, potentially increasing patient comfort by decreasing the work of breathing.[4,10]

Times to 50 and 90% increase include the period of trigger delay and therefore reflect the effect of sensor sensitivity and data processing. Remarkably, due to the physical interaction of volume, resistance, and compliance with decelerating flow during PSV, the time for 50% pressure increase more closely reflects the early response and thus maximal pressurization performance of the devices than the time for 90% pressure increase. Accordingly, we determined the difference between trigger delay and 50% pressurization to discriminate between the devices' performances during pressurization. Investigation of the pressurization performance during volume-controlled ventilation and PCV already demonstrated considerable differences between the devices (supplemental table S3 in part I,[9] https://links.lww.com/ALN/E559). In addition, during PSV, the Carestation consistently showed the fastest pressurization. Interestingly, the Wato did not keep up with the Carestation, although the two devices use the same ventilator technology. Similarly, pressurization differed considerably between the Flow-c and the A9, although both machines drive ventilation by volume reflector technology. Moreover, resistances of the internal inspiratory pneumatic elements of the AWS influence pressurization performance but could not be determined by the current experimental setup. Airway leakage influenced trigger performance and pressurization in an unpredictable fashion but to a minor extent only. We assume that the fresh gas flow set in these experiments compensated for the relatively low volume deficiency, thus ensuring the devices' performance.

The simulated breathing effort needed was considerably lower than reported in other studies evaluating ventilators for children and adults.[3,4,15,16] Different methodologic approaches in the calculation of the PTP may account for the observed differences. We decided to incorporate the area under the pressure time curve from the start of trigger to the curve's nadir, as we believe that this figure represents the patient's net breathing effort. Other studies calculate the entire area under PEEP[4,15] or additionally include the area under the pressurization curve until a certain point in time.[4,15,16]

During PCV, oxygen rise times varied widely for the different models. This can be attributed to age-dependent differences in the simulated FRC, to the relationship between ventilation minute volume of the model and fresh gas flow, and also to different breathing system volumes in the respective patient categories. Interestingly oxygen rise times did not primarily depend on the relationship between FRC and minute volume. A relevant influence of these factors would have resulted in faster oxygen rise times in smaller patient models at the same fresh gas flow. In contrast, independent of the type of AWS, we observed a considerably slower increase in oxygen concentration in the infant and toddler lung model than in the preterm baby and neonate model at the lowest fresh gas flow. The explanation lies probably in the volume of the breathing system attached to the AWS. Indeed, the volume of the 15-mm-inner-diameter breathing system used in the infant and toddler model has more than double the volume of the 10-mm-inner-diameter system used in the smaller models, given the same length.

Overall, the best improvement of oxygen rise occurred when increasing fresh gas flow to 3 $l \cdot min^{-1}$. A fresh gas flow of 3 $l \cdot min^{-1}$ already exceeded the range of delivered patient minute volumes in our study (0.5 to 2.3 $l \cdot min^{-1}$).[9] Consequently, only a moderate increase in fresh gas flow was sufficient to accelerate oxygen concentration rise in the lung model.

Device-specific differences in oxygen rise times necessitate the discussion of variation in system volumes and different technologies for fresh gas supply. Depending on the ventilator technology in use, the volume of the breathing circuit, which is relevant for changes in gas concentrations, can be much lower than the absolute volume indicated in the manufacturers' information. For example, the absolute circuit volume of the Atlan is 3,440 ml during controlled ventilation. The piston contributes to this figure with 1,500 ml at the most extended position. Setting a pediatric patient category leads to stepwise lowering of the pistons volume to a limit necessary for provision of the set tidal volume. Thus, in the preterm baby model, the effective system volume of the Atlan approximated 1,950 ml after a couple of breaths.

Consequently, the observed long oxygen rise times with the Atlan rather result from the principle of fresh gas

decoupling then from system volume. Fresh gas decoupling in the Atlan diverts flow backwards into the reservoir bag during inspiration. The piston fills from the reservoir bag, and the gas is transported in portions corresponding to the set tidal volume. Although this approach provides an advantage in terms of tidal volume precision,[9] changes in gas composition require equilibration of the gas concentrations in the reservoir bag and the piston.[17] Consequently, the oxygen increase is delayed and depends on tidal volume but not on fresh gas flow. This can be derived from the saturation curves in the Atlan, the courses of which are independent of the fresh gas flow.

The Perseus showed the lowest absolute system volume but long oxygen rise times at a fresh gas flow of 1 l · min^{-1} in all models. For the Perseus, the fresh gas flow is fed continuously into the breathing circuit but is separated into a forward flow to the patient and a reverse flow to the turbine. Thus, distribution of fresh gas flow depends on the resistive counter pressures from each direction of flow. Times to change gas concentration in the breathing circuit rather depend on fresh gas flow than on tidal volume in this device. The Perseus's low circuit volume promoted an initial steep rise in oxygen concentrations. However, the low backward-directed fresh gas flow impedes proper gas mixing in the volume of the ventilation bag, which serves as a reservoir in the circuit. Emptying of the poorly saturated reservoir starts late at low set minute volume, which leads to the late flattening of the oxygen concentration curve in the preterm baby model. With the higher minute volume (but the same breathing hose volume) in the neonate model, emptying of the reservoir starts earlier, which leads to an earlier decrease in the rate of rise of the oxygen concentration. When further increasing the minute volume, these effects become insignificant, resulting in an overall good performance as also demonstrated in models of adult patients.[17] As a clinical consequence, using a short breathing bag hose and an appropriately small breathing bag in the Atlan and the Perseus may be advantageous in terms of time required to increase oxygen concentration, particularly with low tidal volumes.

The Carestation and the Wato inject fresh gas into the circuit between the ventilator and the inspiratory limb (please see fig. 1 in the accompanying article[9]). Although the point of injection is similar to that of the Perseus, inspiratory fresh gas flow is only directed forward in these devices. The breathing bag is not part of the circuit during automatic ventilation. Accordingly, changes in oxygen concentration were generally faster. To enable precise control of the tidal volume, the volume accelerated by the bellow is reduced by the amount of fresh gas flow. This accounts for approximately one third of the set fresh gas flow given an inspiratory to expiratory ratio of 1:2. The ratio between fresh gas flow and patient minute volume thus determines the speed of gas concentration rise. The slightly faster rise in oxygen concentration with the Carestation compared to the Wato may be a consequence of the difference in delivered minute volume. Comparison of precision of PCV revealed that with the same ventilator settings as applied in the experiments for gas changing times, the Carestation generated up to 15% more minute ventilation, which is attributable to an inaccuracy of the inspiration time regulation.[9]

The Flow-c and the A9 performed oxygen rise times in the middle, although their system volumes were the lowest of all devices. Moreover, from the volume of the Flow-c reflector (1,200 ml) and the A9 reflector (1,500 ml), only a portion equaling the set tidal volume contributes to functional system volume during controlled ventilation. Differences between both AWSs may be explained by regulation of the fresh gas flow. In the preterm baby model, the oxygen rise time with the Flow-c was slower than with the A9, but it was faster at higher minute volumes. In the Flow-c, a fresh gas flow exceeding the patient's minute volume is automatically down-regulated to match this figure for more efficient gas usage. Minute volumes were about 0.5 l · min^{-1} in the preterm baby and 0.8 l · min^{-1} in the neonate model. Consequently, we could observe faster oxygen rise times with the neonate compared to the preterm baby model but no improvements in both models with increasing fresh gas flow. In contrast, increasing fresh gas flow at higher minute volumes allow for a more efficient rise in oxygen concentration, without needing to increase the flow above 2.3 l · min^{-1} in our study.

Testing the hypothesis that activation of the oxygen flush button can accelerate an increase in oxygen concentration in the lungs yielded important information. In the Atlan and the Perseus, the oxygen flush accelerated the oxygen concentration in the lungs compared to static fresh gas flow in most cases. Fresh gas decoupling and backwards filling of the breathing circuit, as discussed above, may explain faster oxygen enrichment in the ventilation bag. In the Flow-c, cyclic ventilation was discontinued. An electronically controlled safety function opens the exhalation valve to maintain the current PEEP value. Due to the absence of filling and emptying of the lungs, we could not detect a relevant change in oxygen concentration.

In the Wato and the A9, the oxygen flush function did not lead to a relevant improvement of oxygen rise times considering all patient models and fresh gas flows. However, activation of the oxygen flush increased airway pressures in these devices to a relevant extent. The difference between airway and pulmonary pressure indicates the resistive pressure drop across the pediatric endotracheal tubes,[18] which in this case attenuates overinflation of the lungs. After the initial pressure rise, flow is regulated down, resulting in decreasing peak pressure and PEEP over a couple of breaths. By contrast, the Carestation continuously increased PEEP and decreased driving pressure while the oxygen flush was active. As a result, oxygen concentration rise times were worse than in comparison to 3 and 10 l · min^{-1} fresh gas flow.

It is important to note that the oxygen flush function is intended to serve for a brief refilling of the breathing

circuit only. Therefore, the flush button is designed to be self-closing and to minimize unintended operation.[19] Our results show that its use during pediatric ventilation can lead to dramatically high pulmonary pressures and does not result in a relevant improvement in oxygenation. Therefore, it is strongly discouraged during pediatric ventilation.

With regard to the potential for technical development, our results suggest that the ideal AWS for pediatric ventilation should contain a low system volume and allow for using low-volume breathing hoses. A flow sensor covering a pediatric range and positioned close to the airway device may be advantageous regarding precision of measured and displayed volumes and response times to breathing efforts.[20] The combination with a mainstream carbon dioxide sensor can improve end-expiratory carbon dioxide measurements and would enable volumetric capnography, with its potential for clinical decision-making beyond setting of ventilator parameters.[21,22] The combination of precise and fast volume acceleration, leakage compensation, and low time constants for gas concentration changes may be best achieved with a ventilator driven by an injection valve. However, our results demonstrate that this technology has to be well integrated in the circuit. The oxygen flush function could be disabled in the mechanical ventilation mode. Alternatively, the generated peak flow should be downregulated depending on the set patient category. Display of continuously calculated tracheal pressure is technically feasible and would allow for better estimating the pressure reaching the patient's lungs, particularly during pressure-regulated ventilation.[18]

There are few options for users to overcome the technical limitation of the AWSs evaluated in our study, when used in small children. However, most above-mentioned technical advantages are already available in ventilators for specific use in neonates. Accordingly, the intraoperative use of a neonatal intensive care ventilator should be considered in the most vulnerable patients. Modern drugs for sedation and analgesia may allow for intravenous maintenance of anesthesia even in preterm babies.[23] Active humidification may support appropriate humidity and temperature of the breathing gas.[24] Above that, an increasing number of neonatal ventilators can be used during transport, eliminating the risk of changes in alveolar ventilation caused by switching between ventilators with different performances.[25] Moreover, with a neonatal intensive care ventilator, high-flow nasal oxygen may become available for airway management and procedures performed under sedation.[26]

Anesthesia workstations behave differently when it comes to the ventilation of young children. Standardized comprehensive device tests were unable to identify a specific system that performed best in this respect. Knowledge of the devices' individual strengths and shortcomings may support clinical treatment, risk management, and investment decisions. Moreover, these results could encourage manufacturers to push ahead with their developments in the field of pediatric ventilation.

Research Support

Support was provided solely from institutional and/or departmental sources.

Competing Interests

Dr. Spaeth received a fee as a speaker at a workshop on pediatric ventilation financed by the Dräger Medical Company (Luebeck, Germany) during the 15th European Congress on Pediatric Anesthesiology in Berlin, Germany, in 2025. Dr. Schumann received funding from the Deutsche Forschungsgemeinschaft (Bonn, Germany). The other authors declare no competing interests.

Correspondence

Address correspondence to Dr. Spaeth: Hugstetter Strasse 55, 79106 Freiburg, Germany. johannes.spaeth@uniklinik-freiburg.de

Supplemental Digital Content

Table S1, https://links.lww.com/ALN/E562
Figure S1, https://links.lww.com/ALN/E563
Figure S2, https://links.lww.com/ALN/E564

References

1. Spaeth J, Schumann S, Humphreys S: Understanding pediatric ventilation in the operative setting: Part I. Physical principles of monitoring in the modern anesthesia workstation. Paediatr Anaesth 2022; 32:237–46. doi:10.1111/pan.14378
2. Lebossé M, Kern D, De Queiroz M, et al.; ADARPEF (Association Des Anesthésistes Réanimateurs Pédiatriques d'Expression Française): Ventilation in pediatric anesthesia: A French multicenter prospective observational study (PEDIAVENT). Paediatr Anaesth 2020; 30:912–21. doi:10.1111/pan.13909
3. Jaber S, Tassaux D, Sebbane M, et al.: Performance characteristics of five new anesthesia ventilators and four intensive care ventilators in pressure-support mode: A comparative bench study. Anesthesiology 2006; 105:944–52. doi:10.1097/00000542-200611000-00015
4. Vignaux L, Piquilloud L, Tourneux P, Jolliet P, Rimensberger PC: Neonatal and adult ICU ventilators to provide ventilation in neonates, infants, and children: A bench model study. Respir Care 2014; 59:1463–75. doi:10.4187/respcare.02540
5. Walsh BK, Smallwood CD: Pediatric oxygen therapy: A review and update. Respir Care 2017; 62:645–61. doi:10.4187/respcare.05245
6. Karlsson V, Sporre B, Fredén F, Ågren J: Randomized controlled trial of low vs. high oxygen during neonatal anesthesia: Oxygenation, feasibility, and

oxidative stress. Paediatr Anaesth 2022; 32:1062–9. doi:10.1111/pan.14519
7. Neumann RP, von Ungern-Sternberg BS: The neonatal lung—Physiology and ventilation. Paediatr Anaesth 2014; 24:10–21. doi:10.1111/pan.12280
8. Feldman JM: Optimal ventilation of the anesthetized pediatric patient. Anesth Analg 2015; 120:165–75. doi:10.1213/ANE.0000000000000472
9. Spaeth J, Trost M, Flamm B, Wenzel C, Schumann S: Anesthesia workstation performance in pediatric ventilation: Part 1. Precision of ventilation. Anesthesiology 2026; 145:942–53. doi:10.1097/ALN.0000000000006149
10. Baumgartner J, Schmidt J, Klotz D, Schneider H, Schumann S, Fuchs H: Trigger performance of five pediatric home ventilators and one ICU ventilator depending on circuit type and system leak in a physical model of the lung. Pediatr Pulmonol 2022; 57:744–53. doi:10.1002/ppul.25791
11. Schumann S, Ucar S, Wenzel C, Spaeth J: Calculating intrinsic positive end-expiratory pressure from end-expiratory flow in mechanically ventilated children—A study in physical models of the pediatric respiratory system. Pediatr Pulmonol 2024; 59:766–73. doi:10.1002/ppul.26828
12. Blokpoel RG, Burgerhof JG, Markhorst DG, Kneyber MC: Patient–ventilator asynchrony during assisted ventilation in children. Pediatr Crit Care Med 2016; 17:e204–11. doi:10.1097/PCC.0000000000000669
13. Blokpoel RGT, Koopman AA, Kneyber MCJ: Flow trigger setting in mechanically ventilated neonates, children and adults: A scoping review. Intensive Care Med Paediatr Neonatal 2024; 2:24. doi:10.1007/s44253-024-00047-0
14. Mirabella L, Cinnella G, Costa R, et al.: Patient–ventilator asynchronies: Clinical implications and practical solutions. Respir Care 2020; 65:1751–66. doi:10.4187/respcare.07284
15. Delgado C, Romero JE, Puig J, et al.: Performance of the new turbine mid-level critical care ventilators. Respir Care 2017; 62:34–41. doi:10.4187/respcare.04938
16. Thille AW, Lyazidi A, Richard JC, et al.: A bench study of intensive-care-unit ventilators: New versus old and turbine-based versus compressed gas-based ventilators. Intensive Care Med 2009; 35:1368–76. doi:10.1007/s00134-009-1467-7
17. Shin HW, Yu HN, Bae GE, et al.: The effect of fresh gas flow rate and type of anesthesia machine on time to reach target sevoflurane concentration. BMC Anesthesiol 2017; 17:10. doi:10.1186/s12871-016-0294-y
18. Spaeth J, Steinmann D, Kaltofen H, et al.: The pressure drop across the endotracheal tube in mechanically ventilated pediatric patients. Paediatr Anaesth 2015; 25:413–20. doi:10.1111/pan.12595
19. Eisenkraft J: The anesthesia machine and workstation, Anesthesia Equipment: Principles and Applications. Edited by Ehrenwerth J, Eisenkraft J, Berry J. Philadelphia, Elsevier-Saunders, 2013, pp 25–63
20. Morgenroth S, Thomas J, Cannizzaro V, Weiss M, Schmidt AR: Accuracy of near-patient vs. inbuilt spirometry for monitoring tidal volumes in an in-vitro paediatric lung model. Anaesthesia 2018; 73:972–9. doi:10.1111/anae.14245
21. Humphreys S, Schibler A, von Ungern-Sternberg BS: Carbon dioxide monitoring in children—A narrative review of physiology, value, and pitfalls in clinical practice. Paediatr Anaesth 2021; 31:839–45. doi:10.1111/pan.14208
22. Karlsson J, Lönnqvist PA: Capnodynamics—Measuring cardiac output via ventilation. Paediatr Anaesth 2022; 32:255–61. doi:10.1111/pan.14329
23. Moultrie F, Durrmeyer X, van den Bosch GE, et al.: Analgesia and sedation in premature infants receiving invasive ventilation: A systematic scoping review. Pediatr Res 2025; [in press]. doi:10.1038/s41390-025-04441-y
24. Schiffmann H, Rathgeber J, Singer D, Harms K, Bolli A, Züchner K: Airway humidification in mechanically ventilated neonates and infants: A comparative study of a heat and moisture exchanger vs. a heated humidifier using a new fast-response capacitive humidity sensor. Crit Care Med 1997; 25:1755–60. doi:10.1097/00003246-199710000-00029
25. Abouzeid T, Perkins EJ, Pereira-Fantini PM, Rajapaksa A, Suka A, Tingay DG: Tidal volume delivery during the anesthetic management of neonates is variable. J Pediatr 2017; 184:51–6.e3. doi:10.1016/j.jpeds.2017.01.074
26. Humphreys S, Schibler A: Nasal high-flow oxygen in pediatric anesthesia and airway management. Paediatr Anaesth 2020; 30:339–46. doi:10.1111/pan.13782